ELSEVIER

Journal of Alloys and Compounds 388 (2005) 104–108

Journal of ALLOYS AND COMPOUNDS

www.elsevier.com/locate/jallcom

Formation and magnetic properties of the RE-based compounds of type $RE_6Fe_{13-x}Al_{1+x}$ (RE = Pr, Sm, Gd)

P.T.L. Minh[a], R.W. McCallum[b], L.H. Lewis[c,*], K.W. Dennis[b], M.J. Kramer[b]

[a] *International Training Institute for Material Science (ITIMS), Hanoi, Vietnam*
[b] *Ames Laboratory, USDOE and Department of Materials Science and Engineering, Iowa State University, Ames, IA 50011, USA*
[c] *Materials Sciences Department, Building 480, Brookhaven National Laboratory, Upton, NY 11973-5000, USA*

Received 8 June 2004; accepted 6 July 2004

Abstract

Selected rare-earth (RE)-based δ-phase compounds of the composition $RE_6Fe_{13-x}Al_{1+x}$ ($1 \leq x \leq 4$) have been prepared and studied to ascertain their role in conveying coercivity to the so-called ferromagnetic bulk metallic glass (BMG) alloys $(RE)_{60}Fe_{30}Al_{10}$. It was found that δ-phase does not exist for RE = Sm or Gd. However, nearly single δ-phase Pr-based compounds of the composition $Pr_6Fe_{13-x}Al_{1+x}$ in a range of Al concentration $1.5 \leq x \leq 3.5$ were successfully synthesized. The antiferromagnetic behavior of the Pr-based δ-phase compounds is clearly seen from temperature-dependent magnetization measurements and the Néel temperature shows a quasi-linear decrease from 320 K to 115 K as x in $Pr_6Fe_{13-x}Al_{1+x}$ is increased from 1 to 4. The observed Al-concentration dependence of the $Pr_6Fe_{13-x}Al_{1+x}$ Néel temperatures is expected to be reflected in the magnetic behavior of the BMG alloys of composition $Pr_{60}Fe_{30}Al_{10}$.

Keywords: Amorphous materials; Magnetic measurement; X-ray diffraction; Coercivity; Delta phase

1. Introduction

In 1996, Inoue and Katsuya announced the development of so-called bulk metallic glass (BMG) alloy rods of 1–12 mm in diameter that possessed appreciable coercivity [1]. The ferromagnetic coercive BMG composition $RE_{60}Fe_{30}Al_{10}$ (RE = Nd or Pr) and related alloys modified by Co [2] and Ce and Si [3] have since generated considerable interest of both applied and fundamental nature because the magnitude of this reported coercivity, up to 0.4 T at room temperature, is in apparent contradiction to the conventional understanding of the relationship between nanostructure and coercivity in amorphous materials. The large coercivities observed for the BMG composition in the vicinity of $RE_{60}Fe_{30}Al_{10}$ (RE = Nd or Pr) have been the subject of a number of investigations, since both a very large anisotropy field and a very strong domain wall pinning mechanism are required to account for the observed coercivity which can exceed 10 T at temperatures below 10 K. While the random anisotropy model [4] may account for the anisotropy field, the nature of the pinning sites in an amorphous material remains unclear. Among other explanations, previous authors have speculated that the RE–Fe–Al bulk metallic glasses possess short-range order which confers coercivity [5]. Others researchers have postulated the idea that ferromagnetic single-domain clusters are responsible for the coercivity [6]. Recently reported results [7,8] obtained by a subset of the present authors from analyses of structural and magnetic data obtained on amorphous melt-spun $Nd_{60}Fe_{30}Al_{10}$ materials have identified the origin of the anomalous magnetic coercivity found in the ribbons, and by extension in the bulk cast form of the alloy, as very small crystalline clusters ("motes"). It was determined that these highly stable nanoscopic aluminide phases affect the short-range order of the system and provide heterogeneous nucleation sites for crystallization as well as determine the coercivity of the alloy. A detailed consideration of the Nd–Fe–Al ternary phase diagram allows the deduction that the observed clusters in

* Corresponding author. Tel.: +1-631-344-2861; fax: +1-631-344-4071.
E-mail address: lhlewis@bnl.gov (L.H. Lewis).

0925-8388/$ – see front matter © 2004 Elsevier B.V. All rights reserved.
doi:10.1016/j.jallcom.2004.07.008

the melt-spun ribbons of the BMG alloy must be closely related to the $Nd_2Fe_{17-x}Al_x$ (2-17), μ- and δ-phases, where the μ-phase is ferromagnetic [9] and the δ-phase is antiferromagnetic and is also referred to as the 6-13-1 phase [9,10]. The $Nd_2Fe_{17-x}Al_x$ and μ-phase are ferromagnetic with Curie temperatures T_C around 300 K and 500 K, respectively [11], whereas the δ-phase orders antiferromagnetically at a Néel temperature T_N near room temperature [10,12]. Thus, the onset of coercivity in the ribbons as well as in the bulk metallic glasses may be explained by an exchange-bias type of magnetic coupling [13] where soft ferromagnetic phases (2-17 and μ-phase) are unidirectionally coupled to the antiferromagnetic δ-phase. Extension of this reasoning leads to the hypothesis that the onset of significant coercivity in melt-spun $RE_{60}Fe_{30}Al_{10}$ ribbons containing different rare-earth (RE) species should scale with the Néel temperature of the primary δ-phase product of solidification.

As a first step to verify the validity of the above-described model, investigation of the magnetic behavior of the polycrystalline δ-phase containing different RE elements was undertaken. Praseodymium and samarium were chosen as representative of the light RE elements, while gadolinium represents the heavy RE elements. Previous studies of the Pr-based δ-phase compound have shown that this phase orders antiferromagnetically at different T_N depending upon the identity of the metalloid element [10]. The aim of the present work is to identify the existence range of the δ-phase in single-phase form and investigate the effect of off-stoichiometry on the magnetic behavior of the prepared samples.

2. Experimental procedures

All samples were made from high purity elements: Pr (99.95%), Sm (99.95%), Gd (99.95%), Fe (99.99%) and Al (99.98%) were arc-melted and annealed under high-purity Ar. The chosen compositions of the Pr-based compound were $Pr_6Fe_{13-x}Al_{1+x}$ (x = 1, 1.5, 3, 3.5, 4) and of the Sm(Gd)-based compounds was $Sm(Gd)_6Fe_{11.5}Al_{2.5}$. Extra Sm was added during synthesis of the charges to compensate for Sm volitization during the arc-melting process. The RE and Fe elements were arc-melted together first, and then the Al was subsequently added; this synthesis sequence was necessary to avoid formation of unwanted refractory compounds. All samples were melted several times to obtain homogeneity. The polycrystalline arc-melted charges were wrapped in Ta foil and sealed under high purity Ar prior to annealing. For differential thermal analysis (DTA), the samples were ground and placed in an Al_2O_3 crucible and measured from room temperature to 1350 °C at a heating rate of 10 °C per min with a strictly controlled oxygen concentration below 100 ppm. The DTA results were employed to determine the appropriate annealing schedules to yield the desired $RE_6Fe_{13-x}Al_{1+x}$ compound in single-phase form. The optimized annealing schedules are described in the next section for each family of samples. Structural characterization of the annealed samples was carried out with X-ray diffraction using a Philips diffractometer and Cu Kα radiation. Lattice parameters were determined by Reitveld refinement. SQUID magnetometry was used to measure the DC magnetization in the temperature range 2 K < T < 400 K in a magnetic field of 10 mT (100 Oe).

3. Results and discussion

DTA measurements were performed for both the as-cast and the annealed versions of the synthesized RE-based samples. The DTA results were correlated with the appropriate equilibrium phase diagrams to determine the identity of the phases present in the samples. Conclusions obtained from the DTA results were confirmed with XRD analysis, and, if appropriate, with magnetometry. As the most successful results were obtained for the Pr-based samples, detailed discussion is focused on data obtained from that material.

3.1. Phase content and structure

The arc-melted Gd-based sample exhibits three clear endothermic peaks with onset temperatures of 1333 K, 1143 K and 1483 K; there are no peaks at low temperature as would be characteristic of an analogue of the δ-phase composition. Careful examination of the equilibrium [Gd–Fe–Al] ternary phase diagram [14] allows the conclusion that all the observed DTA peaks are related to the peritectic decomposition of Al-substituted $(Fe,Al)_2Gd$, $(Fe,Al)_3Gd$ and $(Fe,Al)_{23}Gd_6$ compounds. The inability to form the Gd-based δ-phase is in good agreement with the Handbook of Phase Diagrams [14] and the results of previous publications [10].

The as-arc-melted Sm-based sample shows a DTA endothermic peak with an onset at 893 K, which is hypothesized to be associated with the formation of the δ-phase. A heat treatment procedure was applied to obtain the Sm-based δ-phase compound in single-phase form as follows: the sample was heated from 873 K to 1113 K at a rate of 3 K per h and held at 1113 K for 12 h. The subsequent disappearance of the above-mentioned endothermic signal for the annealed sample suggests that the speculated δ-phase formation in this temperature range has completely occurred. However, X-ray diffraction analysis presents no evidence of this anticipated Sm-based δ-phase. Rather, the X-ray diffraction pattern of the annealed Sm-based sample appears to be related to the $SmFe_2$ compound. It is well known that Sm-based compounds are unstable at high temperature. As the loss of Sm and/or of Sm-based compounds in the arc-melting and homogeneity treatment processes is out of our control, the Sm-based δ-phase could not be obtained in the present work.

As earlier reported by Hu et al. [10], it is well known that the Pr-based δ-phase compound exists in a range of substituted element concentration. To deepen the results of reference [10], in the current study, five compositions were chosen for synthesis of the Pr-based δ-phase compound. A small exotherm at ∼773 K in the DTA signal of the as-cast sample is

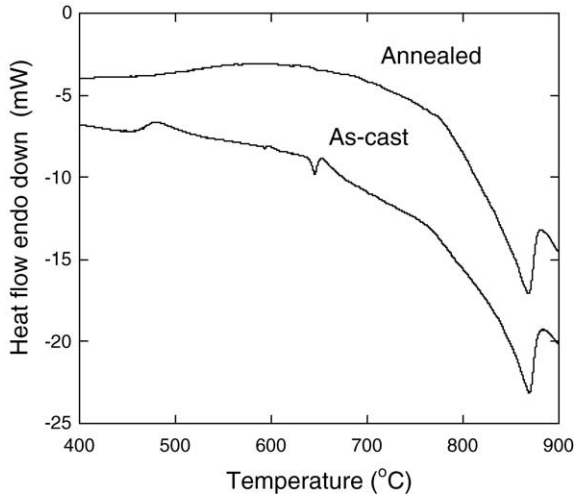

Fig. 1. Representative DTA data of the δ-phase compound $Pr_6Fe_{11.5}Al_{2.5}$ (x = 1.5).

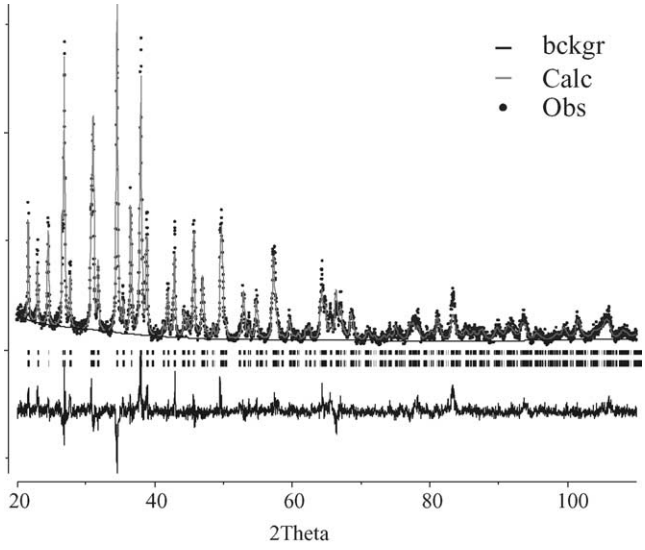

Fig. 2. A refined X-ray diffraction pattern of the annealed Pr-based δ-phase compound $Pr_6Fe_{9.25}Al_{4.75}$ (x = 3.75). The solid lines are JCPDS standard peaks for a powder sample of type $Pr_6Fe_{13}Al$.

obviously related to crystallization. The small peak area indicates that our sample is largely crystalline in its as-cast form. A clear endothermic peak found in the data of the as-arc-melted Pr-based samples (Fig. 1) with an onset at $T \approx 953$ K is anticipated to be related to the formation of the Pr-based δ-phase in the melting process. Thus, an annealing schedule was optimized for the Pr-based samples: the samples were heated from 848 K to 1023 K with a heating rate of 3 K per h and then held at temperature for 12 h. The disappearance of this endothermic peak in DTA signal for annealed Pr-based samples of composition x = 1.5 is evidence that δ-phase formation has completed while the x = 1 sample still possesses evidence of the presence of another phase.

The X-ray diffraction patterns of the Pr-based samples indicate that all the synthesized compositions, except for the x = 1 sample, are single-phased within detection limits and have the crystal structure of type $Pr_6Fe_{13}Si$ (i.e., the δ-phase). A representative XRD pattern is shown in Fig. 2, along with the standard Bragg reflection positions for the 6-13-1 δ-phase obtained from reference [15]. The determined lattice parameters are listed in Table 1. Examination of the variation of the unit cell parameters as a function of Al concentration reveals that the lattice expands with increasing Al content. This observed expansion is attributed to the substitution of Fe by Al atoms and is in agreement with the fact that the atomic radius of Al (0.144 nm) is larger than that of Fe (0.124 nm) [16]. It is concluded from XRD studies that the nominal single δ-phase region extends from $x \sim 1.25$ to $x \sim 3.5$.

3.2. Magnetic character

The magnetization M versus temperature T curves for all five synthesized samples of the Pr-based δ-phase compound are shown in Fig. 3. It can be seen that the Pr-based samples with x = 1.5, 3, 3.5 and 4 are typical antiferromagnets with an antiferromagnetic magnetic ordering Néel temperature T_N identified as a cusp in the signal. The magnetic signal of the x = 1 sample is more atypical and appears to be somewhat ferromagnetic, with a magnetic transition temperature of 320 K; the mixed magnetism of this sample is consistent with its noted two-phase character, identified with DTA and XRD. The low magnetization value found in samples with x = 3, 3.5 and 4 for T > 200 K suggests a fully antiferromagnetic structure. The M versus T curve for the x = 4 sample of the Pr-based sample series exhibits several magnetic transitions and is displayed fully in the inset of Fig. 4. The magnetic behavior of the x = 4 sample includes two ferromagnetic ordering transitions at T = 40 K and 390 K and sharp peak in the magnetization at T = 115 K. The 10-fold increase of the magnetization of the x = 4 sample at low temperature suggests that the observed transition originates from a ferromagnetic impurity. The [Pr–Fe–Al] equilibrium ternary phase diagram provides information to identify this ferromagnetic impurity. It is known that the $Pr_2(Fe,Al)_{17}$

Table 1
Some characteristics of the δ-phase compound $Pr_6Fe_{13-x}Al_{1+x}$

x	Compound	Fe:Al ratio	T_N (K)	a (Å)	c (Å)	Cell volume (Å^3)
1.0	$Pr_6Fe_{12}Al_2$	6.0	320	8.119 (4)	23.202 (9)	1529.64 (3)
1.5	$Pr_6Fe_{11.5}Al_{2.5}$	4.6	300	8.143 (6)	23.151 (1)	1535.34 (0)
3.0	$Pr_6Fe_{10}Al_4$	2.5	175	8.188 (8)	23.139 (7)	1551.66 (6)
3.5	$Pr_6Fe_{9.5}Al_{4.5}$	2.1	135	8.165 (3)	23.059 (5)	1537.42 (6)
4.0	$Pr_6Fe_9Al_5$	1.8	115	8.234 (4)	23.183 (4)	1571.95 (8)

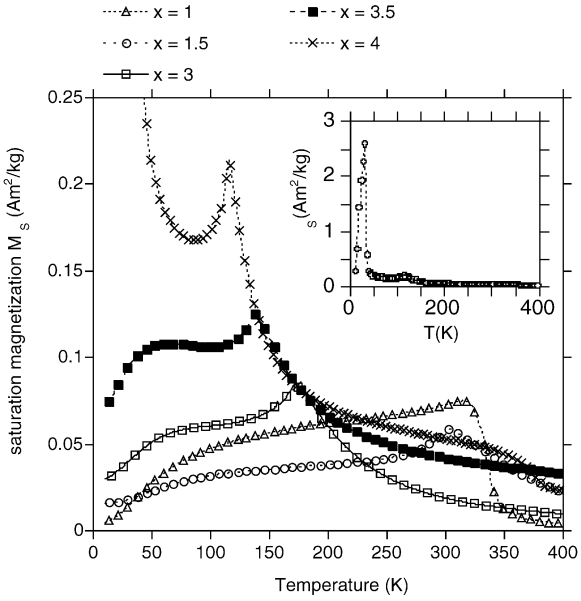

Fig. 3. Magnetization vs. temperature curves for Pr-based δ-phase compounds $Pr_6Fe_{13-x}Al_{1+x}$. The inset shows the full curve for the compound with $x = 4$.

compound orders ferromagnetically at the Curie temperature T_C in the range $295\,K \leq T_C \leq 420\,K$ depending on the amount of Al substituted into the structure [17,18]. Thus, the observed ferromagnetic transition at $T = 390\,K$ for the $x = 4$ Pr-based sample is likely from a very small amount of the 2:17 Al-substituted phase. The other ferromagnetic transition is attributed to the presence of the $PrAl_2$ compound which orders ferromagnetically at $T_C \sim 38\,K$ [19]. The concurrence in magnetizations of these ferromagnetic phases and the antiferromagnetic δ-phase may mask the antiferromagnetic transition of the δ-phase resulting in the observed peak at 115 K.

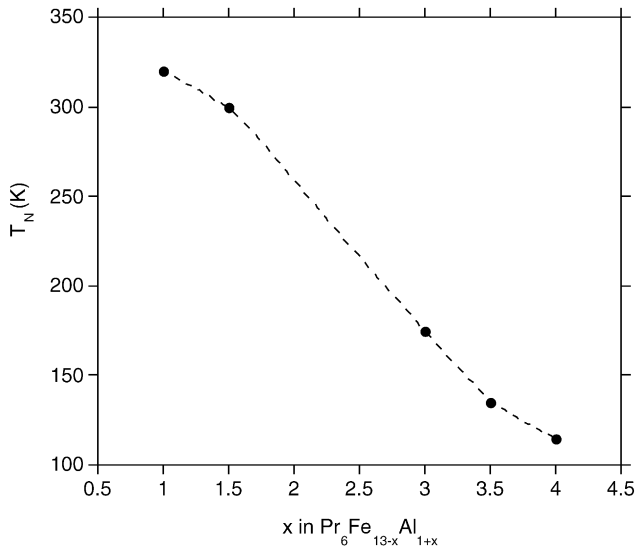

Fig. 4. Al-concentration dependence of the Néel temperatures for Pr-based δ-phase compounds $Pr_6Fe_{13-x}Al_{1+x}$. Dashed line connecting data markers serves to guide the eye.

For intermediate values of x, the magnetization data also show evidence of ferromagnetic impurities. As mentioned earlier, the DTA data of the $x = 1$ composition show evidence of an impurity. Interpretation of the magnetization data for this sample suggests that the ferromagnetic transition of the hypothesized 2:17 impurity phase with $T_C \sim 300\,K$ overwhelms the antiferromagnetic transition signal of the δ-phase of composition $Pr_6Fe_{12}Al_2$ with T_N near this temperature, leading to the observed behavior of the measured M versus T curve.

The dependence of the measured $Pr_6Fe_{13-x}Al_{1+x}$ Néel temperatures T_N upon Al concentration is graphed in Fig. 4 and it is clear that the Néel temperature decreases strongly with increasing Al content from about 115 K ($x = 4$) to about 320 K ($x = 1$). It is hypothesized that the presence of the nonmagnetic Al atom dilutes the antiferromagnetic coupling existing between the RE elements and the Fe sublattice and thereby decreases the T_N. As discussed above, all five samples of the Pr-based material were found to contain a 2-17-type ferromagnetic impurity that may mask the AF ordering signal of the δ-phase. A detailed investigation on the Al-concentration dependence of the Curie temperature of the Pr_2Fe_{17} ferromagnetic phase is underway in order to give better interpretation to the Al-concentration dependence of the T_N of the current studied compounds.

4. Conclusions

We have shown that in the ternary RE–Fe–Al system, the $RE_6Fe_{13}Al$ compound does not form for RE = Gd and Sm. However, the $Pr_6Fe_{13-x}Al_{1+x}$ δ-phase was detected in all compositions synthesized from $1 \leq x \leq 4$. In the compositional region of $1.5 \leq x \leq 3.5$, the antiferromagnetic Néel temperature T_N varies quasi-linearly from 320 K to 115 K. Based on the proposed model of magnetic behavior of BMG-type alloys of composition $RE_{60}Fe_{30}Al_{10}$ [6], both the formation of the BMG alloys and the development of their high coercivity are attributed to the primary solidification product in the compositional region of interest, the δ-phase $RE_6Fe_{13}Al$, with the Fe:Al ratio controlled by the starting alloy composition in the BMG formation region. The obtained experimental results obtained on Pr-based compounds of the δ-phase are anticipated to contribute to basic understanding of the magnetic properties of the RE-based ferromagnetic BMG materials. Further investigation of the correlation between the observed magnetic properties of the δ-phase and those of the corresponding melt-spun vitrified ribbons is needed to perfect the picture of the "Bulk Metallic Glass".

Acknowledgements

Research was performed under the auspices of the U.S. Department of Energy, at Ames Laboratory under Contract No. W-7405-ENG-82 and at Brookhaven National Laboratory under contract No. DE-AC02-98CH10886. Support

from the East Asia and Pacific Program of the Division of International Programs, N.S.F., is gratefully acknowledged.

References

[1] A. Inoue, A. Katsuya, Mater. Trans. JIM 37 (1996) 1332.
[2] B.C. Wei, Y. Zhang, Y.X. Zhuang, D.Q. Zhao, M.X. Pan, W.H. Wang, W.R. Hu, J. Appl. Phys. 89 (6) (2001) 3529.
[3] H. Chirac, N. Lupu, J. Magn. Magn. Mater. 196–197 (1999) 235.
[4] E. Callen, Y.J. Liu, J.R. Cullen, Phys. Rev. B16 (1) (1977) 263.
[5] Inoue, A. Takeuchi, T. Zhang, Metal. Mater. Trans. A 29A (1998) 1779.
[6] H.Z. Kong, J. Ding, L. Wang, Y. Li, IEEE Trans. Magn. 37 (4) (2001) 2500.
[7] R.W. McCallum, M.J. Kramer, K.W. Dennis, L.H. Lewis, Proceedings of the 17th International Workshop on Rare-Earth Magnets and Their Applications, August 18–22, Newark, Delaware, USA, 2002.
[8] M.J. Kramer, A.S. O'Connor, K.W. Dennis, R.W. McCallum, L.H. Lewis, L.D. Tung, N.P. Duong, IEEE Trans. Magn. 37 (2001) 2497.
[9] B. Grieb, E.T. Henig, G. Martinek, H.H. Stadelmaier, G. Petzow, IEEE Trans. Magn. 26 (1990) 1367.
[10] B. Hu, J.M.D. Coey, H. Klesnar, P. Rogl, J. Magn. Magn. Mater. 117 (1992) 225.
[11] J. Delamare, D. Lemarchand, P. Vigier, J. Magn. Magn. Mater. 104–107 (1992) 1092–1093.
[12] F. Weitzer, A. Leither-Jasper, P. Rogl, K. Hiebl, H. Noel, G. Wiesinger, W. Steiner, J. Solid State Chem. 104 (1993) 368–376.
[13] J. Nogues, I.K. Schuller, J. Magn. Magn. Mater. 192 (1999) 203.
[14] Handbook of Ternary Alloy Phase Diagrams, Copyright 1995 by ASM International.
[15] F.W. Wang, J. Magn. Magn. Mater. 177 (1998) 1056.
[16] J.F. Shackelford, W. Alexander (Eds.), Materials Science and Engineering Handbook, CRC Press LLC, Boca Raton, FL, 2001.
[17] F. Weizer, K. Hiebl, P. Rogl., J. Appl. Phys. 65 (12) (1989) 4963–4967.
[18] F. Weizer, H. Klesnar, K. Hiebl, P. Rogl, J. Appl. Phys. 67 (5) (1990) 2544–2548.
[19] K.H. Mader, E. Segal, W.E. Wallace, J. Phys. Chem. Solids 30 (1) (1969) 1–12.